Cellular Polymers 13, 1–15 1994

Experimental Study of Size Effects and Surface Damage in Closed-Cell Polymethacrylimide and Open-Cell Copper Foams

W.B. Anderson, C.P. Chen, PhD, Postdoctoral Researcher and
R.S. Lakes, PhD, Professor

Department of Mechanical Engineering,
Department of Biomedical Engineering,
University of Iowa,
Iowa City, IA 52242, USA

SUMMARY

This article describes experimental investigations of size effects in torsion and bending of lathe cut closed-cell polymethacrylimide and open cell copper foams. Slender specimens were found to have a slightly smaller effective stiffness than thick ones. This behaviour is consistent with a model of surface damage to the outermost cells of the foam. The surface damage layer was inferred to be from 0.13 to 0.37 cell diameters for the polymethacrylimide, depending on the grade of foam, and from 0.3 to 0.4 cells in the copper foam. Effects of Cosserat (micropolar) elasticity, which would give rise to an effective stiffening of slender specimens, were not observed.

1. INTRODUCTION

Local inhomogeneity in cellular materials arises from the relatively large structure of their cells. It is true that even "solid" materials have structure at the atomic level; however, this structure is usually ignored and the materials are assumed continuous in engineering applications. This assumption has proven satisfactory for many engineering materials such as solid metals, polymers, ceramics and glasses. However, with foams and many other composite materials, the structure becomes large enough that the assumption of continuity comes into question. In fact, classical elasticity theory has been a poor predictor of fracture behaviour and stress concentrations around holes and cracks in many fibre composites and foams. Experimental stress concentrations in composites are consistently lower than predicted classically[1]. The shortcomings of classical theory suggest that either the composite materials should no longer be assumed continuous, or that a more general elasticity theory may be appropriate.

Cosserat Elasticity

The question of how much freedom is to be incorporated in an elasticity theory must be decided by experiment. For classical isotropic elasticity, the constitutive equation is given by[2,3]

$$\sigma k l = \lambda \varepsilon_{rr} \delta_{kl} + 2G \varepsilon_{kl} \quad (1)$$

in which there are two independent elastic constants λ and G.

More freedom is incorporated in the Cosserat theory of elasticity, also known as micropolar elasticity[4,5,6,7]. This theory incorporates a local rotation of points as well as the translation assumed in classical elasticity; and a couple stress (a torque per unit area) as well as the force stress (force per unit area). The force stress is referred to simply as 'stress' in classical elasticity in which there is no other kind of stress. In the isotropic Cosserat solid there are six elastic constants, in contrast to the classical elastic solid in which there are two. Certain combinations of Cosserat elastic constants have dimensions of length and are referred to as characteristic lengths. The constitutive equations for a linear isotropic Cosserat elastic solid are:

$$\sigma k l = \lambda \varepsilon_{rr} \delta_{kl} + (2\mu + \kappa)\varepsilon_{kl} + \kappa \varepsilon_{klm}(r_m - \phi_m) \quad (2)$$

$$m_{kl} = \alpha \phi_{r,r} \delta_{kl} + \beta \phi_{k,l} + \gamma \phi_{l,k} \quad (3)$$

The usual summation convention for repeated indices is used throughout. σ_{kl} is the force stress, which is a symmetric tensor in Equation (1) but it is asymmetric in Equations (2) and (3). m_{kl} is the couple stress, $\varepsilon_{kl} = (u_{k,l} + u_{l,k})/2$ is the small strain, u_k is the displacement, and e_{klm} is the permutation symbol. The microrotation ϕ_k in Cosserat elasticity is kinematically distinct from the macrorotation $r_k = (e_{klm}u_{m,l})/2$. In three dimensions, the isotropic Cosserat elastic solid requires six elastic constants λ, μ, α, β, γ, and κ for its description.

One consequence of Cosserat elasticity theory is that a size-effect is predicted in the torsion and bending of circular cylinders of Cosserat elastic materials. The effective stiffness associated with such cylinders increases as their size decreases[8,9]. A similar size effect is also predicted in the bending of plates[8] and beams[9]. This size-effect has led to an experimental method for determining the Cosserat elastic constants of a material[1,10,11].

Size effect studies on human bone disclosed Cosserat type effects, and the characteristic length for bone was obtained[10]. It has also been found that size effects consistent with the Cosserat continuum view occur in

several polymer foams. All six Cosserat elastic constants were determined for a polyurethane foam[11]. As for dynamical behaviour of foam materials, dispersion of standing waves and cut-off frequencies were observed experimentally. It was found that foamed materials did not obey the classical theory of elasticity or viscoelasticity[12].

The physical cause of Cosserat elasticity in foams and fibrous materials is the bending and twisting moment carried by the structural elements. A spatial average of these moments represents the couple stress in. 3.

Non-local Elasticity

Another generalized continuum theory that has been proposed for the analysis of materials with microstructure is nonlocal elasticity. Here the stress at a point depends not only on the strain at that point, but on the strain in a region near that point. The constitutive equation for an isotropic nonlocal solid is[13]

$$\sigma_{ij}(x) = \int_V \{ \lambda(|x'-x|)\, \varepsilon_{rr}(x')\, \delta_{ij} + 2\mu(|x'-x|)\varepsilon_{ij}(x') \}\, dV(x') \qquad (4)$$

A simpler representation is

$$\sigma_{ij}(x) = \int_V \{\alpha(|x'-x|)\, [\lambda\varepsilon_{rr}(x')\, \delta_{ij} + 2\mu\varepsilon_{ij}(x')]\, dV(x') \qquad (5)$$

with the nonlocal kernel $\alpha(|x|)$ subject to $\int_V \alpha(|x|)dV = 1$, requiring the kernel to be a member of a Dirac delta sequence. So, in the limit of the non-local distance of influence or characteristic length, a, associated with the kernel a becoming vanishingly small, the classical Hooke's law is recovered.

As with Cosserat elasticity, there is a size effect predicted in bending and torsion with nonlocal elasticity. There also is predicted a size effect in tension. However, the size effect in nonlocal solids may be opposite to that in Cosserat solids, i.e., the apparent elastic moduli would decrease with decreasing specimen size. Lakes[13] showed that this phenomenon arises in bending, torsion and tension when, near the surface, only a portion of the kernel's region of influence is integrated over, and, hence contributes to the stress. Thus, if the kernel is positive definite throughout its range, then there is a surface layer of depth a in which the stress is less than $E\varepsilon$. If the kernel is not positive definite, and goes negative over part of its range, then there may be a stiffening effect of small specimens. So nonlocal elasticity theory allows both the apparent increase in modulus with decreasing specimen size (as with Cosserat elasticity) and the apparent decrease in modulus with decreasing specimen size.

The physical mechanism underlying nonlocal elasticity is long range cohesive force. An example is the electromagnetic force between ions in a crystal. In foams and fibrous systems, the generation of long range forces is not so easy to visualize.

Edge Effects

An alternative to the above continuum views and their associated physical processes is the structural view of edge or surface effects. In a foam, the cells at the edge of an item are incomplete. Moreover, some cells may be damaged by the cutting process. These edge cells contribute to the volume of the specimen, but are not able to carry much load. Hence, the effective stiffness of the specimen is less than what would be expected. This effect becomes more pronounced as the specimen size approaches the cell size.

An edge effects model was developed by Brezny and Green[14] for bending of a square cross section beam. The model is based on the idea that a layer exists on the outer portion of the specimen composed of incomplete and/or damaged cells. This layer contributes to the volume of the specimen, but not to the stiffness. The beam can be modelled as a composite of two materials: an inner core of material 1 with modulus E_1 and an outer layer of material 2 with modulus E_2, where $E_2 < E_1$. The thickness of the layer of incomplete (and/or damaged) cells remains constant regardless of specimen size, and may be larger or smaller than one cell size. Thus, as specimen size is reduced, and the ratio of incomplete to complete cells increases, the apparent stiffness decreases.

The beam may be considered as one material, given the same resistance to bending by reducing the width of each element of modulus E_2 by the factor $n = E_2/E_1$. Now, the moment of inertia, I, can be calculated using the transfer of axis theorem for each section. Assuming a beam of unit cross section, the moment of inertia is given by[14]

$$I = \frac{(1-2X+2nX)(1-2X)^3}{12} + \frac{2nX^3}{12} + nX(1-X)^2 \qquad (6)$$

where X is the thickness of the layer of incomplete cells.

The model for round specimens is an extension of that for square specimens. Consider a beam of diameter d containing an outer layer of thickness X of incomplete cells. The moment of inertia for the beam is

$$I_o = \left(\frac{\pi}{64}\right)d^4 \qquad (7)$$

The beam can be thought of as a composite with the inner portion consisting of material 1 with moment of inertia I_1 and modulus E_1 (and G_1). The outer layer consists of material 2 with moment of inertia I_2 and modulus E_2 (and G_2). To obtain the same resistance to bending in the outer layer while using material 1, we need a moment of inertia I_3 such that

$$E_2 I_2 = E_1 I_3 \tag{8a}$$

or

$$I_3 = \frac{E_2}{E_1} I_2 \tag{8b}$$

So, for an equivalent beam made entirely of material 1,

$$I_e = I_1 + I_3, \tag{9a}$$

or

$$I_e = \frac{\pi}{64}\left\{(d-2X)^4 (1-n) + nd^4\right\} \tag{9b}$$

where the modulus ratio $n = \frac{E2}{E1}$

The relative modulus, E_e/E_o, may be calculated. Now, E_e is the modulus of the sample measured experimentally and E_o is the modulus of a sample of the same material but accounting for edge effects. Thus, E_e assumes that $I = I_o$, since the entire specimen is considered to contribute to the modulus, while E_o is determined with $I = I_e$, assuming a value for incomplete layer thickness X, and for n approaching 0. E_o, therefore, is the modulus of material with the same cell size, but exhibiting no edge effects. These two moduli are described by

$$E_e = \frac{ML}{\delta I_o} \tag{10a}$$

$$E_o = \frac{ML}{\delta I_e} \tag{10b}$$

Hence, the relative modulus is equivalent to the relative moment of inertia:

$$\frac{E_e}{E_o} = \frac{I_e}{I_o} = \left(\frac{1}{d^4}\right)\left\{(d-2X)^4(1-n)+nd^4\right\} \tag{11}$$

Similar analyses of round and square specimens in torsion yield the same results as above for relative polar moment of inertia and relative shear modulus.

Some of the data reported by Brezny and Green[14] suggested that the incomplete cell layer thickness for larger cell size material is less than the cell size. They also point out that in small cell size materials, there may be additional factors such as machining damage that could cause the layer thickness to appear to be larger than one cell size.

It is the purpose of this study to investigate the size effects in foamed materials by experiment. The effective shear modulus and Young's modulus of closed-cell polymethacrylimide and open-cell copper foams of different densities and sizes were obtained from torsion and bending tests upon specimens of different thickness.

2. MATERIALS AND METHODS

In a classically elastic rod, the bending and torsion rigidity are proportional to the fourth power of the diameter. In a thin plate the bending rigidity is proportional to the third power of the thickness. The rigidity depends on size in a different way in Cosserat elastic materials: thin specimens are more rigid than would be expected classically. It is possible to determine one or more of the Cosserat elastic constants by measurements of specimen rigidity vs size. This approach, which we call the method of size effects, has been used in many experimental efforts both old and recent[1,10,11]. In non-local solids, thin specimens may be more rigid or less rigid than expected classically. If surface effects are dominant, thin specimens will also be less rigid than expected classically.

The size effects tests were conducted on cylindrical Rohacell® polymethacrylimide foam and cylindrical copper foam. Three grades of Rohacell were tested, WF51, WF110 and WF300 (CYRO industries), corresponding to different densities. Rohacell® is a closed-cell foam of typical cell morphology with average cell size l_{cell} approximately from 200 μm to 500 μm, as observed using the scanning electron microscope (SEM). The variation of the cell size l_{cell} of the foams was found to exist in each individual foam specimen, and not to exhibit any significant dependence on the foam density. For the WF51 and WFl 10, specimens were cut from a foam block of their grades. For foam WF300, specimens were cut from two different foam blocks, designated A and B. The densities of the specimens cut from different blocks were somewhat different. For grades WF51, WF110 and WF300 of block A, specimens were cut with a lathe. For foam WF300 of block B, specimens were cut

with a lathe, then smoothed with emery paper to improve surface finish. The densities and final sizes of the specimens are given in Table 1.

The copper foam consists of open cells of tetrakaidecahedral shape and fairly regular cell size. Two cell sizes were tested, 1.3 mm (20 pores per inch) and 0.64 mm (40 pores per inch), with relative densities of 0.039 and 0.053, respectively. Both round and square specimens were machined. The round specimens were first rough cut into square blocks with an end mill, then machined round by lathe, with a counter-rotating deburring tool. The deburring tool consisted of a carbide cylinder, 19 mm in diameter with 26 teeth that spiral down the cylinder. The lathe speed was 1350 rpm and the deburring tool speed was 24,000 rpm in the opposite direction. This combined for relative surface cutting speeds of 24.5 to 25 mls, at 173 cuts per second. Further reductions in specimen size were obtained with the lathe and deburring tool; the end of the specimen held in the lathe collet was removed after each machining so that further compression of the foam did not occur. This method provided a consistent cross-section for the specimens and limited cell strut breakage and material smearing.

The experiments were conducted using a micromechanics apparatus at room temperature (20°C to 23°C). The experimental method and its data reduction was used for study of viscoelastic solids and polymeric foams, and given in detail in earlier publications[15,16]. Briefly, an

Table 1 Specimen sizes and densities

Grade of foam	Specimen diameter (mm)	Specimen length (mm)	Density (g/mm ^{3})
WF51	12.6	58.5	0.056
	11.0	43.5	0.056
	7.69	40.5	0.056
	7.22	35.8	0.056
	4.40	21.7	0.056
WF110	12.7	51.0	0.11
	6.15	23.6	0.11
	4.70	16.5	0.11
WF300 (Block A)	11.2	47.4	0.34
	7.86	40.9	0.34
	7.18	36.6	0.34
	6.59	31.5	0.34
	5.21	26.4	0.34
	4.40	20.0	0.34
WF300 (Block B)	12.7	51.5	0.32
	6.40	24.8	0.30
	3.25	23.1	0.29

experimental apparatus and analysis scheme for determining the viscoelastic properties of a material isothermally, with a single apparatus, over 10 decades of time and frequency were developed. The range of equivalent frequency for torsion is from less than 10^{-6} Hz to about 10^{4} Hz. Torque was applied to the specimen electromagnetically. A Helmholtz coil under current control acted upon a magnet fixed to the specimen free end (Figure 1). Specimen deformation was determined by laser interferometry in which a laser beam passed through a grating, reflected off a mirror fixed to the specimen end and through another grating into a light detector. All specimens in this study were loaded in torsion, only the WF110 and the copper specimens were loaded in bending. The apparatus is capable of creep, constant load rate, sub-resonant dynamic, and resonant dynamic experiments in bending and torsion. The tests were conducted at 0.1 Hz for this study. At this low frequency, the results were considered to be static and free from the dynamic effects since the specimens' resonances were found to be as high as above 5 kHz.

Figure 1 Schematic diagram of experimental apparatus

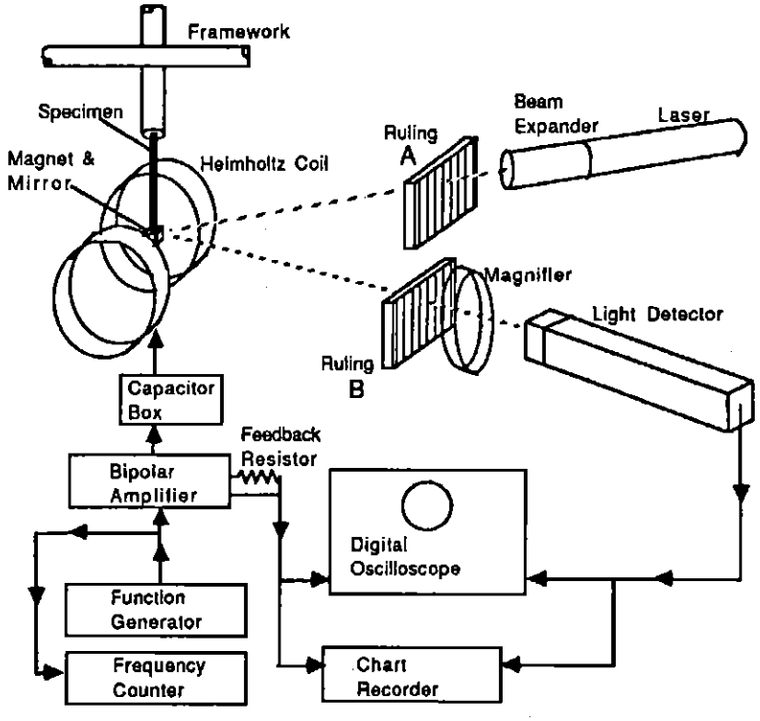

3. RESULTS AND DISCUSSION

To display the size effect data, it is convenient to plot rigidity divided by the square of the diameter against the square of the diameter. For a classically elastic material, the plot should be a straight line through the origin, since the rigidity depends on the fourth power of the diameter in both torsion and bending. For a Cosserat elastic material, the plot should be a curve offset above the classical curve by an amount related to the characteristic length. Edge effects produce the opposite effect, an "anti-Cosserat" softening that causes the curve to be offset below the classical curve, as in the analytical curves in Figure 2.

The results of the polymethacrylimide tests are shown in Figure 3 for torsion and Figure 4 for bending. The rigidity divided by the square of the diameter, J/d^2, against the square of the diameter, d^2, for the various grades are shown. It was found that for grade WF300, the deviation in rigidity for specimens cut from two different foam blocks is negligible. The data points can be fitted reasonably well using a linear curve fit with the shear modulus G = 40 MPa for grade WF51, 75 MPa for WF110 and 360

Figure 2 Analytical size effects curves for rods in bending or torsion under several assumptions. Rigidity divided by square of diameter vs square of diameter, assuming E = 28 MPa. Classical elasticity gives a straight line through the origin. Cosserat elastcity, which incorporates moments carried by cell ribs, gives a stiffening effect of small specimens. Surface damage or incomplete surface cells give a softening effect.

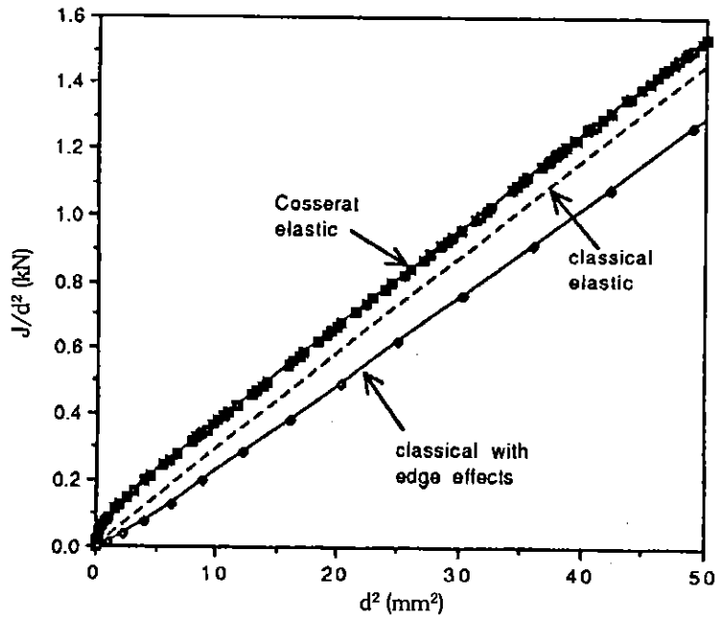

MPa for WF300, and Young's modulus, E = 213 MPa for WF110 in bending. However, it is indicated that there is no evidence of Cosserat elasticity for any of the foam specimens since their effective moduli tend to decrease as diameters decrease. This is consistent with edge effects as in Figure 2. It is possible that there are Cosserat phenomena occurring, but that at the small sample sizes, edge effects are dominating. The edge effects tend to compete with the Cosserat size effects in a test such as this.

Figures 3 and 4 show the data with a classical curve fit represented by a dashed line, and an edge effects curve fit represented by a solid line. The best fit edge effects curves were obtained using the modulus values above, and minimizing the residual error. The residual error here is defined as the sum of the squares of the deviations of the data from the model. For the edge effects analysis, the damage layer X was assumed to provide no stiffness to the specimen, hence the modulus ratio, n, was taken to be zero. The WF51 was found to be nearly classical in torsion, with the best fit edge effects curve giving a value of X = O within the experimental uncertainty.

Figure 3 Torsional rigidity divided by the square of the diameter, J/d^2, against the square of the diameter, d^2, Rohacell® foam, experiment. Classical (dashed line) and best fit edge effects (solid line) curves are shown.
◊: WF51; Δ: WF110; o: WF300, block A; o: WF300, block B

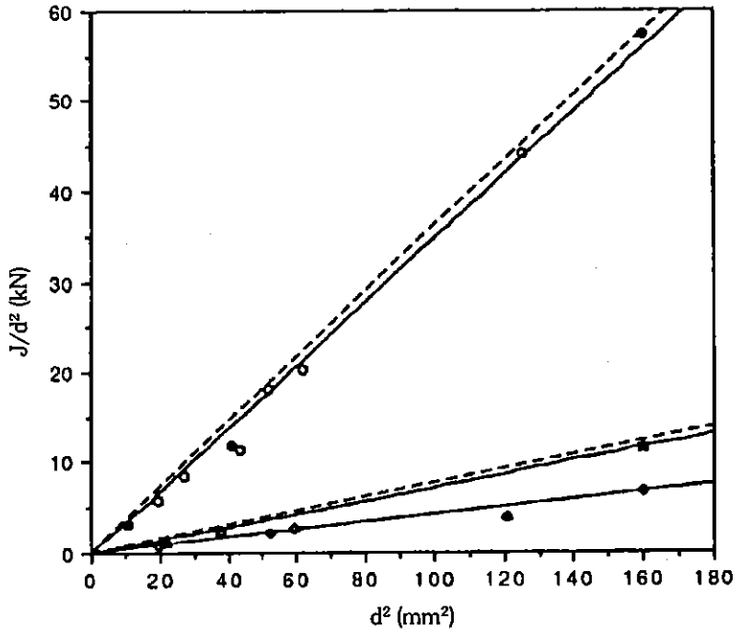

Figure 4 Bending rigidity divided by the square of the diameter, J_b/d^2, against the square of the diameter, d^2, Rohacell® foam WF110, experiment. Classical (dashed line) and best fit edge effects (solid line) curves are shown

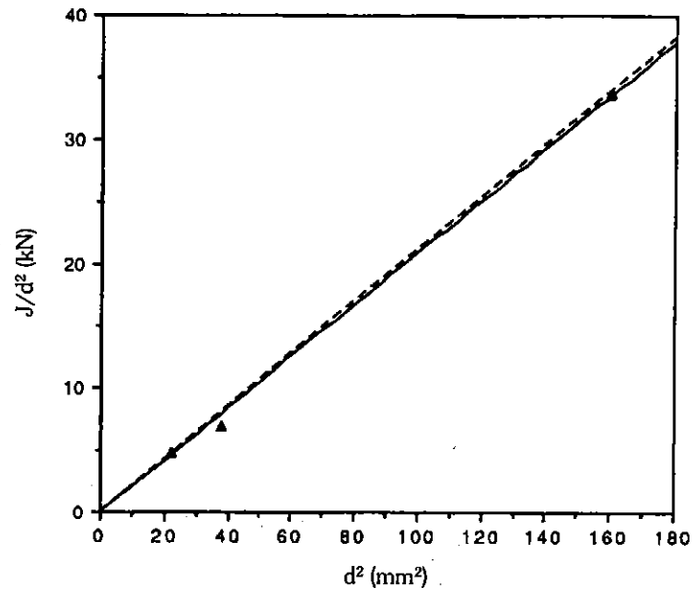

The best fit edge effects curves for WF110 gave values of X = 0.078 mm (0.37 cells) in torsion and X = 0.027 mm (0.13 cells) in bending. The residual error for the edge effects curve in torsion was 0.0933 kN^2 and in bending was 0.979 kN^2. The classical curves gave residual errors of 0.556 kN2 and 1.44 kN^2 in torsion and bending, respectively. The edge effects model, therefore, reduces the residual error by 83% in torsion and 32% in bending for the WF110.

The best fit edge effects curve for WF300 gave X = 0.053 mm (0.11 cells) in torsion The residual error for the edge effects curve was 1.95 kN^2 and for the classical curve was 8.41 kN^2. The edge effects model gives a 77% reduction in residual error over the classical curve.

Edge effects may result from damage to the cells on the surface of the specimen, as well as from incomplete cells. The specimens in this study were all machined on a lathe, with no special precautions taken to avoid surface damage. The WF300 specimens from block B were lightly abraded with emery paper following lathe machining. It may be possible to avoid the surface effects by more careful machining, such as by a light abrasive method. For specimens with sufficiently large size or better surface treatment, the effect on the results due to incomplete or damaged surface cells would be reduced.

Results for the round copper foam specimens appear to show edge effects dominating their behaviour, as seen in Figures 5 and 6. In the figures, the solid curve represents the edge effects model for a classical material. The Young's modulus and shear modulus for the foams were determined using the Gibson and Ashby model for open cell foam[17] and a Young's modulus for solid copper of 110 GPa[18]. For the 1.3 mm cell size, this gives E = 167 MPa, G = 63 MPa, and, assuming a modulus ratio n = 0, a damage layer thickness X = 0.35 cells (0.4 mm) from the torsion data and X = 0.4 cells (0.5 mm) from the bending data (Figure 5). These values for X agree well considering the scatter in the data. The residual error for the edge effects curve was 0.104 kN^2 in torsion and 1.07 kN^2 in bending. The classical curves residual errors were 9.80 kN^2 in torsion and 89.0 kN^2 in bending.

The 0.64 mm cell size foam was calculated to have E = 309 MPa, G = 116 MPa, and a damage layer thickness X = 0.3 cells in both bending and torsion, assuming n = O (Figure 6). The residual error for the edge effects curve was 1.06 kN^2 in torsion and 4.94 kN^2 in bending. The classical curves residual errors were 14.0 kN^2 in torsion and 49.4 kN^2 in bending.

Figure 5 Size effects results for 1.3 mm cell size round copper foam in torsion (open squares) and bending (solid diamonds). Solid lines represent edge effects model with damage layer X = 0.35 cells in torsion and X = 0.4 cells in bending. Dashed lines are classical elastic curves

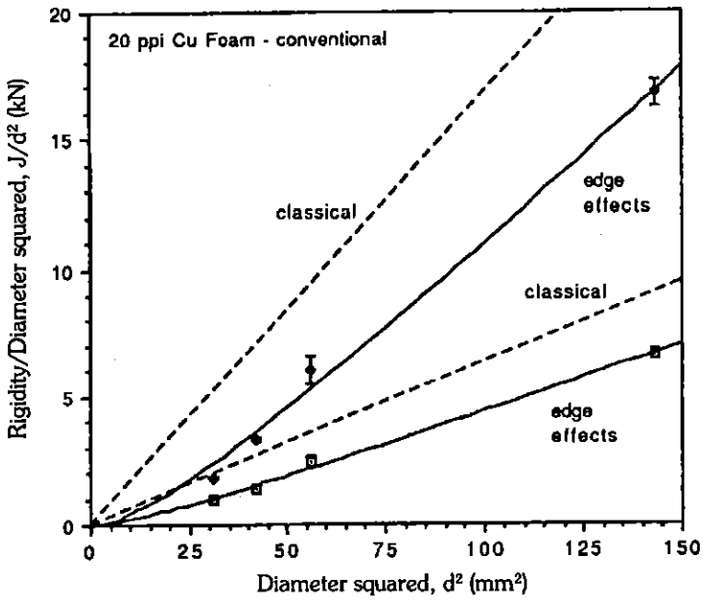

Figure 6 Size effects results for 0.64 mm cell size round copper foam in torsion (open squares) and bending (solid diamonds). Solid lines represent edge effects model with damage layer X = 0.3 cells in both torsion and bending. Dashed lines are classical elastic curves

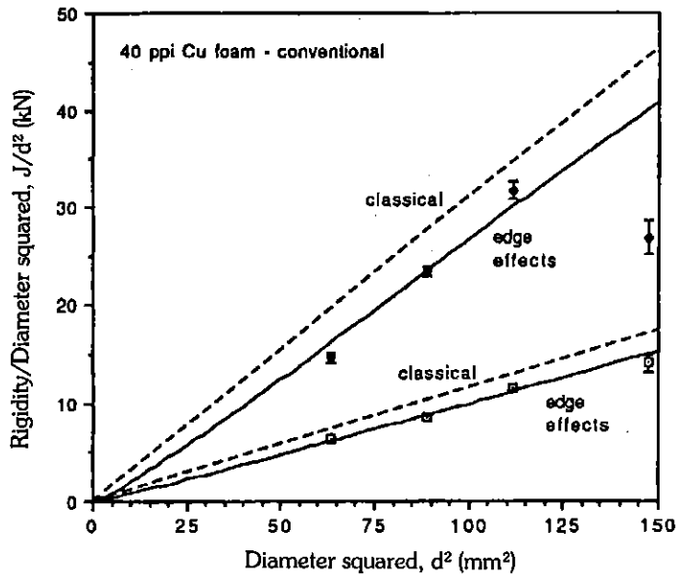

The fact that surface effects dominate the behaviour of the copper foam may in part be attributable to machining damage. The foam is very difficult to work with since it is so ductile. The scatter in the data suggests that the damage was not consistent from machining to machining. In addition, some specimens were broken during machining, suggesting that even those that weren't broken underwent substantial loading that may have caused some of the outer cell ribs to yield. The cell size of the copper foam is also quite large, such that even at the largest specimen size there were only about 10 cells across for the 1.3 mm foam and 20 cells across for the 0.64 mm foam. Brezny and Green recommend at least 15 to 20 cells across an edge to avoid edge effects[14].

In this study, the damage layer was assumed to contribute no stiffness to the specimen. This seems reasonable for the open cell foam, however, for a closed cell foam such as Rohacell®, the contribution of the faces in the damage layer is not obvious. It is possible that partial faces joining the ribs of the incomplete cells may impart some stiffness to the damage layer. In that case, the modulus ratio n could no longer be assumed to be zero, and the thickness of the damage layer would be larger. It is also important to note that the damage layer is not a constant thickness along the

specimen edge. The value of X, therefore, represents a sort of average layer thickness for the specimen.

4. CONCLUSIONS

The size effect behaviour in lathe cut closed cell Rohacell® polymer foams and of open cell copper foam is consistent with a model of surface damage to the outermost cells of the foam. The layer thickness of damaged and/or incomplete cells was inferred to be from 0.13 to 0.37 cell diameters, depending on the grade of Rohacell® foam, and from 0.3 to 0.4 cells in copper foam. No effects of Cosserat (micropolar) elasticity, which would give rise to an effective stiffening of slender specimens, were observed.

ACKNOWLEDGEMENT

The support by Northrop Corporation of this work is gratefully acknowledged. We also thank NASA for partial support via the Boeing/ATCAS program.

REFERENCES

1. Lakes R.S., "Experimental micro mechanics methods for conventional and negative Poisson's ratio cellular solids as Cosserat continua", J. of Engineering Materials and Technology, Vol. 113, 1991, 148
2. Sokolnikoff I.S., Mathematical Theory of Elasticity, Krieger, 1983
3. Fung Y.C., Foundations of Solid Mechanics, Prentice Hall, 1968
4. Cosserat E. and Cosserat F., Theorie des Corps Deformables, Hermann et Fils, Paris, 1909
5. Eringen A.C., Theory of micropolar elasticity. In Fracture, Vol. 1, 621, (edited by H. Liebowitz), Academic Press, 1968
6. Cowin S.C., "An incorrect inequality in micropolar elasticity theory", J. Appl. Math. Phys. (ZAMP), Vol. 21, 1970, 494
7. Mindlin R.D., "Stress functions for a Cosserat continuum", Int. J. Solids and Structures, Vol. 1, 1965, 265
8. Gauthier R.D. and Jahsman W.E., "A quest for micropolar elastic constants", J. Applied Mechanics, Vol. 42, 1975, 369
9. Krishna Reddy G.V. and Venkatasubramanian N.K., "On the flexural rigidity of a micropolar elastic circular cylinder", J. Applied Mechanics, Vol. 45, 1978, 429

10. Yang J.F.C. and Lakes R.S., "Transient study of couple stress effects in human compact bone", J. Biomechanical Engineering, Vol. 103, 1981, 275
11. Lakes R.S., "Experimental microelasticity of two porous solids", International Journal of Solids and Structures, Vol. 22, 1986, 55
12. Chen C.P. and Lakes R.S., "Dynamic wave dispersion and loss properties of conventional and negative Poisson's ratio polymeric cellular materials", Cellular Polymers, 9, 1989, 343
13. Lakes R.S., "How to experimentally distinguish Cosserat and non-local materials", Boeing technical report, 1993
14. Brezny R and Green D.J., "Characterisation of edge effects in cellular materials", J. Materials Science, Vol. 25, 1990, 4571
15. Shipkowitz A.T., Chen C.P. and Lakes R.S., "Characterisation of high-loss viscoelastic elastomers", J. Materials Sci., 23, 1988, 3660
16. Chen C.P. and Lakes R.S., "Apparatus for determining the viscoelastic properties of materials over ten decades of frequency and time", J. Rheology, 33, 8, 1989, 1231
17. Gibson L.J. and Ashby M.F., Cellular Solids: Structure and Properties, Pergamon Press, Elmsford, NY, 1988
18. Van Vlack L.H., Materials for Engineering, Addison-Wesley, Reading, Mass, 1982

CELLULAR POLYMERS

VOLUME 13 1994

EDITOR

J.M. BUIST

EDITORIAL ASSISTANT

KATE EVANS

Published by

RAPRA
TECHNOLOGY LTD.

Information Publications